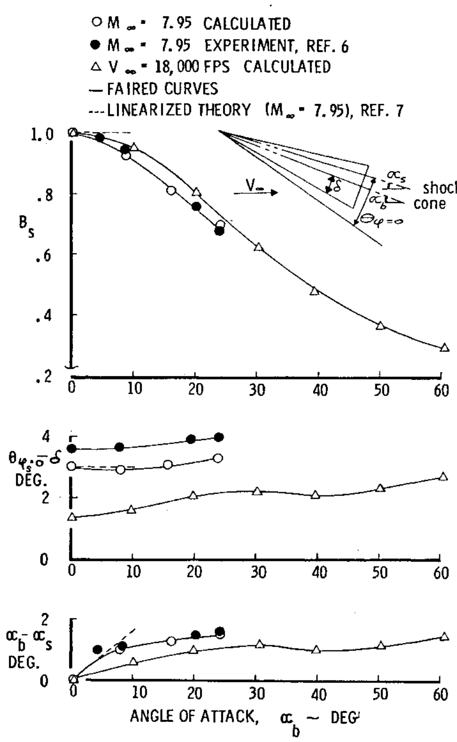

Fig. 4 Comparison of calculated and experimental shock shape parameters: $\delta = 10°$.

Figure 5 shows lines of constant temperature, density, entropy, and pressure in the windward shock layer of the cone at an angle of attack of 60°.

The shock-shape parameters plotted in Fig. 4, as well as additional results not presented here, indicate the following:

1) The difference between the body and shock wave angle of attack ($\alpha_b - \alpha_s$) is small, so that once the desired body angle of attack is specified the shock angle of attack can be accurately estimated. Thus, B_s and $\theta_{\varphi_s=0}$ are essentially the only unknowns that must be estimated to define the shock shape.

2) $\theta_{\varphi_s=0}$ does not vary rapidly with angle of attack. The value for zero angle of attack can be used as an initial estimate.

3) At zero angle of attack the shock shape is circular and therefore, $B_s = 1$. With increasing angle of attack the shock shape becomes more elliptical, and the value of B_s decreases. (B_s was found always to have the same general variation, so that after gaining some experience accurate values could easily be estimated.)

For all results, the assumption that the shock shape could be estimated by the equation for a conic was found to be valid.

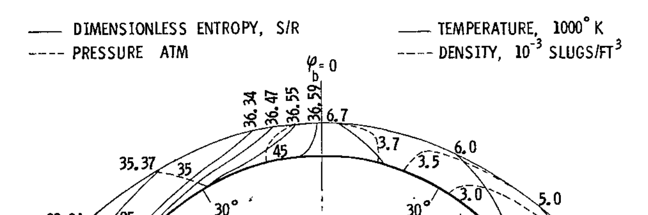

Fig. 5 Variation of shock layer properties for a 10° half-angle cone at 60° angle of attack: V_∞ = 18,000 fps and h = 50,000 ft.

References

[1] Hayes, W. D. and Probstein, R. F., "Hypersonic flow theory," (Academic Press, New York, 1959), p. 230.

[2] Stocker, P. M. and Mauger, F. E., "Supersonic flow past cones of general cross-section," J. Fluid Mech. **13**, 383–399 (1962).

[3] Van Dyke, M. D. and Gordon, H. D., "Supersonic flow past a family of blunt axisymmetric bodies," NASA TR R-1 (1959).

[4] Eastman, D. W., "Real gas flow fields about highly yawed cones by the inverse method," Boeing Co. Doc. D2-20447-1 (1964); available through the Defense Documentation Center AD 450 287.

[5] Hansen, C. F., "Approximations for the thermodynamic and transport properties of high-temperature air," NASA TR R-50 (1959).

[6] Tracy, R. R., "Hypersonic flow over a yawed circular cone," Guggenheim Aeronautical Laboratories, California Institute of Technology, GALCIT Memo. 69 (1963).

[7] Sims, J. L., "Tables for supersonic flow around right circular cones at small angles of attack," NASA SP-3007 (1964).

A Random Signal Multiplier for Turbulence Measurements

V. Kruka*

Syracuse University, Syracuse, N. Y.

In the study of turbulent diffusion of a scalar quantity such as temperature it is of interest to investigate correlations of velocity-temperature fluctuations. These correlations are necessary for balancing the perturbed energy and higher order temperature correlation equations. The latter is obtained by multiplying the turbulent energy equation by the temperature fluctuations and averaging over time. The result gives a relation between convection, production, and dissipation of temperature fluctuations. The double correlations found in the energy equation are easily determined by conventional means. The higher order temperature correlation equation, however, gives rise to triple correlations such as $\langle\theta^2 u_i\rangle$, where θ and u_i represent temperature and velocity fluctuations, respectively. It is for the evaluation of these quantities that the random signal multiplier was designed.

Physically, these correlations are measured by means of a 3-wire hot-wire probe, with the wires placed in the usual X-array but with two wires parallel to each other. For temperature fluctuation measurements one of the parallel wires is at an overheat ratio, the ratio of hot to cold resistance, different from the others. The various mean voltage products $\langle e_i e_j e_k\rangle$ obtained from the three wires determine the desired double and triple correlations. Often, for the purpose of temperature fluctuation measurements, it has been customary to assume that a wire at a low overheat ratio behaves as a resistance thermometer, whereas one at a high overheat ratio responds only to velocity changes. The errors introduced with this assumption are not always negligible. For instance, in the case of tungsten wires, with an upper practical overheat ratio limit of 1.8, subjected to 10% turbulence and 2°F rms temperature fluctuation, 20% of the signal from the wire is due to temperature effects. Platinum wires with their inherently higher possible overheat ratios will improve but not avoid the approximation. The multiplier removes this source of error by allowing for sensitivity to both velocity and temperature on all wires.

A schematic circuit diagram of the random signal multiplier discussed here is shown in Fig. 1. The device is based

Received June 8, 1965. This work was supported by the National Science Foundation under Grant No. GP-354.

* Research Associate, Department of Mechanical and Aerospace Engineering.

on the quarter-square principle, i.e.,

$$e_1e_2 = \tfrac{1}{4}[(e_1 + e_2)^2 - (e_1 - e_2)^2]$$

The squaring in this instance is performed by electron beam deflection tubes (Raytheon QK329) as first proposed by Miller et al.[1] For operation, these tubes require $\pm\ (e_1 + e_2)$ and $\pm\ (e_1 - e_2)$. The inverters at the multiplier input provide $\pm\ e_1$ and $\pm\ e_2$, which are then combined into the desirable form by the summing network. The summing is achieved by a simple, passive resistance network that has a gain of 0.3. The behavior of the beam deflection tubes is poor for small voltages, so that the output of the summing network is boosted by a factor of 10 in the amplification stage. Amplification at this point in the circuit requires four additional operational amplifiers. A similar increase in the signal level could be achieved by only two amplifiers at the multiplier input. However, for the particular operational amplifiers employed here (Philbrick, Inc., amplifiers) this procedure would have overdriven the inverters. Provision for adjustable capacitors is found necessary on the input resistors of the amplification stage to compensate for stray capacitances in the preceding circuitry. Since a precise mechanical centering of the electron beam in the beam deflection tube is impossible, it must be achieved electronically through external circuitry. The biasing on the amplification stage serves this purpose. The output of the beam deflection tubes provided at the targets is at a level elevated above that acceptable to the subtractor. Furthermore, the level of the two tubes need not be necessarily equal. The biased reduction network preceding the cathode follower balances the two tubes and brings the signal near ground level. The cathode follower prevents the drawing of excessive currents from the beam deflection tubes. After the final operation, the subtraction, the output has an over-all gain of $\frac{1}{5}$, a value that is determined by the choice of resistances in the circuitry. The time-mean of the product is easily obtainable; application of the multiplier output to a simple resistance-capacitance "integrating" network of the appropriate time constant

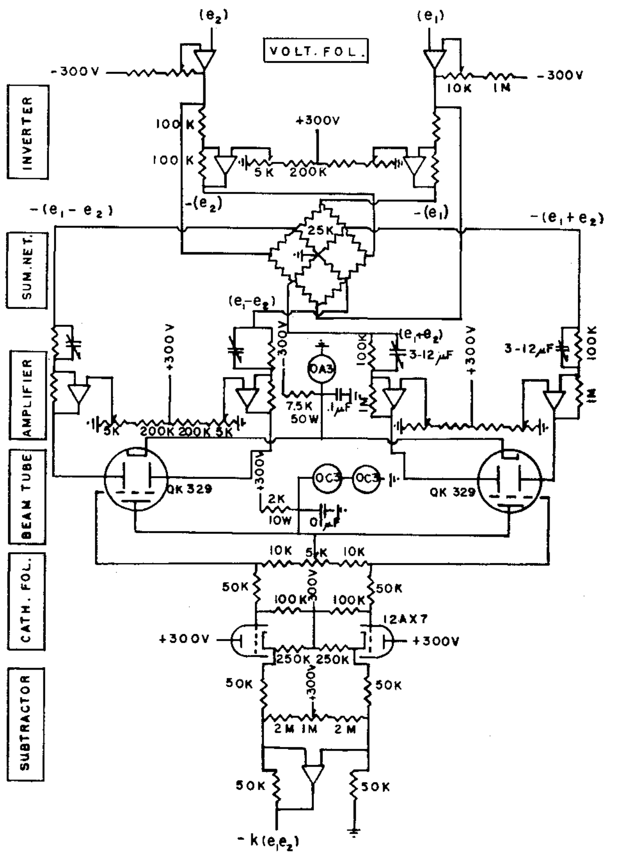

Fig. 1 Multiplier schematic circuit diagram.

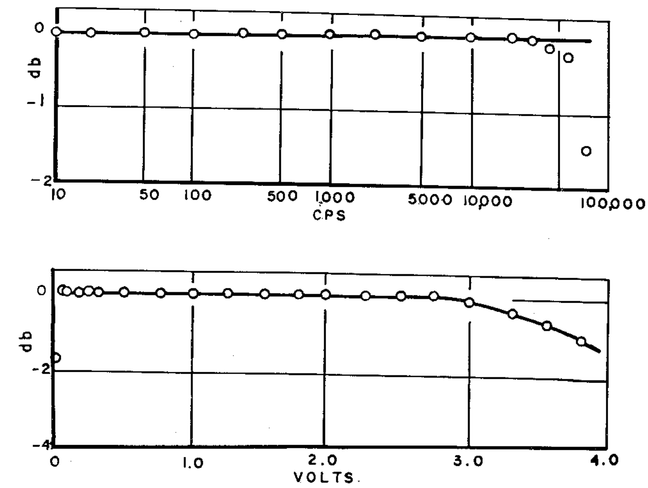

Fig. 2 Multiplier frequency and amplitude response.

and observation of the "integrator" output on a high impedance electronic d.c. voltmeter will give the desired value.

In constructing the multiplier care has to be exercised in the choice of some of the circuit elements. The resistors in the summing network and around the operational amplifiers are of the film type, offering small internal capacitance and inductance. This precaution minimizes distortion due to phase shifts. For the purpose of avoiding distortion due to amplitude differences, these resistors are also matched to within 0.02%. Cost considerations led to the use of unstabilized operational amplifiers. Performance and ease of operation would be enhanced by stabilized amplifiers; in particular they would remove the need for long warm-up times and bothersome biasing adjustments. The output of the beam deflection tubes is affected by small changes in all internal voltages. To avoid errors due to supply voltage variations, the cathode and plate voltages are kept at a constant −75 and +220v d.c., respectively, by voltage regulating tubes. In addition all heating currents are regulated. Use of filters on the cathode and plate supply to remove a.c. ripple and use of d.c. heating currents yielded a low final noise figure of 200μv referred to the output. As the beam deflection tubes are not shielded by the manufacturer, the electron beam will be deflected by spurious external fields unless protected by the user. Finally, the input impedance of the multiplier is too low for conventional hot-wire anemometers, so that voltage followers have been added at the input for impedance matching.

Initial circuit adjustments are easy to perform once it has been determined that the gains of the voltage followers, inverters, and subtractors are unity, whereas those of the amplification stage are equal to each other. After sufficient warm-up time the voltage followers and inverters are biased for zero d.c. shift. Then the adjustable capacitors of the amplification stage are set for zero phase shift between the multiplier input and the amplification stage output. This is achieved by first letting $e_1 = e_2 = E \sin\omega t$ and adjusting the capacitors on the $\pm\ (e_1 + e_2)$ amplifiers, then allowing $e_1 = -e_2$ and correcting the remaining two capacitors. To center the beam deflection tubes again let $e_1 = e_2$, display $(e_1 + e_2)$ vs Ke_1e_2, and adjust either one of the $(e_1 + e_2)$ amplification stage biases till both legs of the displayed parabola have the same height. The same procedure, after letting $e_1 = -e_2$, is followed for the $(e_1 - e_2)$ amplifiers. It might be necessary to repeat the last two steps several times. The reduction circuit after the beam deflection tubes must be balanced such that the attenuation and signal level is equal on both $(e_1 + e_2)^2$ and $(e_1 - e_2)^2$. This is achieved by adjusting the 5000 ohm pot until a linear relation exists between e_1 and the output for $e_2 = 0$. Finally the subtractor bias is set for zero output under the condition of $e_1 = e_2 = 0$.

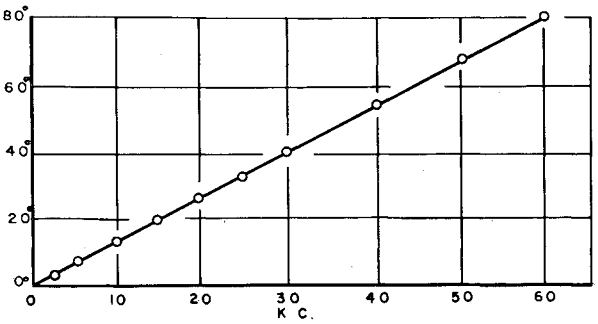

Fig. 3 Multiplier phase lag.

The performance of the multiplier, as indicated in Fig. 2, seems satisfactory for turbulence measurements. The frequency response was obtained under the most strenuous conditions, the squaring of a sine wave which involves doubling of the input frequency. The response is acceptable up to 50 kc, a value rarely exceeded in subsonic flows. A 50 fold range, flat within 0.5 db, is indicated for the amplitude response. There is an undesirable loss in gain near zero input voltage. However, if the signals to be multiplied cover the whole amplitude range, then only an insignificant portion of the desired product is affected. When working with random signals, such as encountered in turbulence measurements, the exact amount of the error is indeterminable since the wave forms and amplitudes are unknown. For the case when $e_1 = e_2 = E \sin\omega t$, the error in the product is 20% for $E = 0.07$ v, only 3% for $E = 0.10$ v, and rapidly goes to zero for increasing E. The gain of the amplification stage determines the usable amplitude range and was chosen to conform with a particular hot-wire anemometer in mind. It can easily be set at any desirable level by change of the feedback resistors.

For measurements of triple voltage products, two multipliers are used in series. Care must then be taken in regards to phase shifts between the first product (e_1e_2) and the new signal e_3. Figure 3 gives the phase lag of the multiplier output as a function of frequency. The phase shift is substantial, but up to 50kc it is linear with frequency. Thus a simple, constant-time delay circuit can be used to put e_3 in phase with the product (e_1e_2).

Reference

[1] Miller, J. A., Soltes, A. S., and Scott, R. E., "Wide-band analog function multiplier," Electronics **28**, 160–163 (1955).

Structure of Gaseous Detonations in a Convergent-Divergent Channel

John H. Lee,* Romas Knystautas,†
and Benedict H. K. Lee‡
McGill University, Montreal, Quebec, Canada

SUFFICIENT evidence has been gathered in recent years to show conclusively that gaseous detonation waves are unstable.[1] The structure of the detonation wave is extremely complex, consisting of localized ignition heads. Combustion spreads in the transverse direction along the shock front and results in a highly turbulent reaction zone. A technique to achieve a laminar detonation was proposed by White[2] utilizing a convergent-divergent channel. The concept behind this technique is to produce a highly overdriven detonation wave in the convergent channel so that the detonation wave in the divergent channel remains sufficiently overdriven to retain a laminar structure, at least as a transient condition. The spark interferogram of White does indicate that a laminar reaction zone was achieved. In this note, some experimental observations of the structure of a gaseous detonation wave propagating in a convergent-divergent channel are reported. Equimolar acetylene-oxygen mixtures were used, and the experiments were performed at subatmospheric initial pressures ranging from 4- to 8-cm Hg.

To observe the structure of the detonation wave, the open-shutter technique was used. The technique is to focus the transparent window of the convergent-divergent channel onto a stationary film. The shutter of the camera is kept open throughout the duration of the experiment, and the aperture is adjusted so that normal burning is not recorded and only the highly luminous ignition heads can cause sufficient exposure on the film. This technique works best when the

Received June 17, 1965.

* Assistant Professor, Department of Mechanical Engineering. Member AIAA.

† Research Engineer, Department of Mechanical Engineering. Member AIAA.

‡ Research Assistant, Department of Mechanical Engineering.

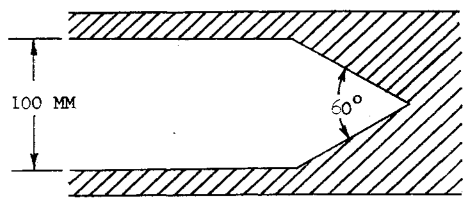

a)

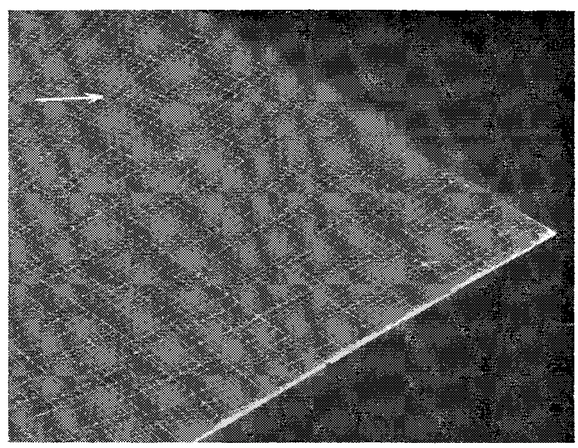

b)

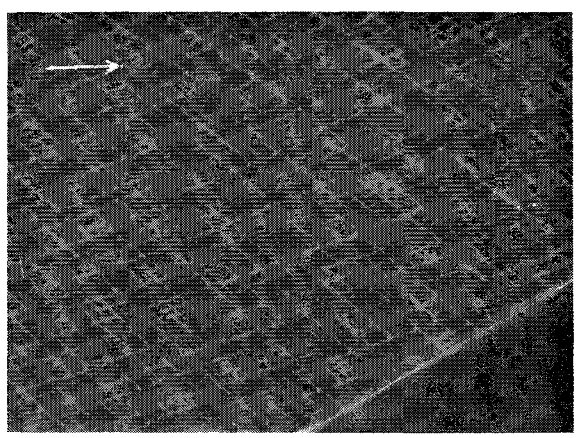

c)

Fig. 1 Open-shutter records of the propagation of a detonation wave in a convergent channel. Equimolar acetylene-oxygen mixture at an initial pressure of 60-mm Hg is used. An enlarged view of the multihead structure of the detonation wave is shown in c). The thickness of the channel is 2 mm. The direction of propagation of the detonation wave is indicated by arrows.